



Using wave intensity analysis to determine local reflection coefficient in flexible tubes



Ye Li^a, Kim H. Parker^b, Ashraf W. Khir^{c,*}

^a Brunel Institute for Bioengineering, Brunel University, Middlesex, UK

^b Department of Bioengineering, Imperial College, London, UK

^c Department of Mechanical Engineering, Brunel University, Middlesex, UK

ARTICLE INFO

Article history:

Accepted 1 June 2016

Keywords:

Arterial waves
Reflection coefficient
Wave intensity analysis
Wave energy

ABSTRACT

It has been shown that reflected waves affect the shape and magnitude of the arterial pressure waveform, and that reflected waves have physiological and clinical prognostic values. In general the reflection coefficient is defined as the ratio of the energy of the reflected to the incident wave. Since pressure has the units of energy per unit volume, arterial reflection coefficient are traditionally defined as the ratio of reflected to the incident pressure. We demonstrate that this approach maybe prone to inaccuracies when applied locally. One of the main objectives of this work is to examine the possibility of using wave intensity, which has units of energy flux per unit area, to determine the reflection coefficient. We used an *in vitro* experimental setting with a single inlet tube joined to a second tube with different properties to form a single reflection site. The second tube was long enough to ensure that reflections from its outlet did not obscure the interactions of the initial wave. We generated an approximately half sinusoidal wave at the inlet of the tube and took measurements of pressure and flow along the tube. We calculated the reflection coefficient using wave intensity (R_{di} and $R_{di}^{0.5}$) and wave energy (R_i and $R_i^{0.5}$) as well as the measured pressure (R_{dp}) and compared these results with the reflection coefficient calculated theoretically based on the mechanical properties of the tubes. The experimental results show that the reflection coefficients determined by all the techniques we studied increased or decreased with distance from the reflection site, depending on the type of reflection. In our experiments, R_{dp} , $R_{di}^{0.5}$ and $R_i^{0.5}$ are the most reliable parameters to measure the mean reflection coefficient, whilst R_{di} and R_i provide the best measure of the local reflection coefficient, closest to the reflection site. Additional work with bifurcations, tapered tubes and *in vivo* experiments are needed to further understand, validate the method and assess its potential clinical use.

© 2016 The Authors. Published by Elsevier Ltd. This is an open access article under the CC BY-NC-ND license (<http://creativecommons.org/licenses/by-nc-nd/4.0/>).

1. Introduction

Earlier work has shown that arterial reflected waves affect the morphology of the arterial pressure waveform in the ascending aorta (Westerhof et al., 1972; Murgu et al., 1980; Khir and Parker 2005). Also, it has been shown that physiological wave reflections have known clinical importance since they contribute to the increase in systolic pressure as seen with the ageing population and hypertensive patients (O'Rourke and Mancia, 1999; Westerhof and O'Rourke, 1995). Further, the timing and magnitude of wave reflection are related to left ventricular relaxation (Yano et al., 2001), vascular stiffness (McEniery et al., 2005) and coronary artery disease (Lekakis, et al., 2006). Furthermore, reflected compression

waves arriving to the ascending aorta during systole may increase left ventricular (LV) mechanical work and oxygen demands (O'Rourke and Hashimoto, 2007).

Several techniques have been proposed to quantify the arrival time (Khir et al., 2007) and magnitude of arterial wave reflection. Murgu et al. (1980) introduced the augmentation index (AIx), although several investigators questioned the capability of this technique to quantify the magnitude of the reflected waves (Westerhof et al., 2006; Lemogoum et al., 2004; McEniery et al., 2005; Segers et al., 2007; Kips et al., 2009; Khir et al., 2006). Further, Westerhof et al. (1972) using a frequency domain technique; impedance analysis, and Parker and Jones (1990) using a time domain technique; wave intensity analysis (WIA) introduced methods based on the simultaneous measurement of pressure and flow at the same site to separate the measured pressure waveform into its forward and backward components and use them to calculate the magnitude of reflection. The results of the two methods are remarkably similar (Hughes and Parker, 2009) and this wave

* Correspondence to: Brunel Institute for Bioengineering, Brunel University, Kingston Lane, Uxbridge, Middlesex UB8 3PH, UK. Tel.: +44 1895265857; fax: +44 1895274608.

E-mail address: ashraf.khir@brunel.ac.uk (A.W. Khir).

separation analysis has been considered the gold standard method to assess wave reflection (Nichols and O'Rourke, 2005, Westerhof et al., 2004).

In wave mechanics of fields such as optics and acoustics, the reflection coefficient is defined as the ratio of the energies of the reflected to the incident wave (Lighthill, 1978). However, in arterial wave mechanics the reflection coefficient for waves is generally defined simply as the ratio of the reflected to the incident pressure wave, since pressure has the units of energy per unit volume. Notwithstanding, there are problems with this approach. For pressure waveforms with a duration T , the 'length' of a wave is equal to cT where c is the wave speed. In the arteries, for example, wave speeds are typically of the order of 10 m/s and the duration of systole is typically 0.3 s, which means that the length of the systolic pressure wave is 3 m; much longer than the length of the aorta. As a result, the forward incident wave and the backward reflected wave overlap giving rise to a complex summation waveform, which may obscure the accurate determination of the reflection coefficient. Hence, it appeared reasonable to replicate the concepts used in the fields of acoustics and optics, and attempt to use an energy-based approach in studying the reflection coefficient in fluid-filled flexible tubes.

Although investigating the use of WIA to quantify the reflection coefficient at discontinuities was carried out computationally (Mynard et al., 2008), experimental validation is lacking. Therefore, the main objective of this study is to investigate whether WIA can be used to determine the local reflection coefficient experimentally in vitro. We also aim to compare the experimental results to the theoretical values obtained using the mechanical properties of the tubes, and to the general definition of reflection coefficient using the measured pressure.

2. Methods

2.1. Experimental setup

The general experimental setup of this work is shown in Fig. 1 and a description of the individual elements is as follows:

2.1.1. Tubes

In this work we used one "mother" silicon tube, which is 3 m long, 10 mm internal diameter and 1 mm wall thickness, and 6 "daughter" tubes of different sizes and materials, each 14 m long. These lengths were needed to allow for investigating a single reflection generated at the discontinuity between the mother and daughter tubes without the added complexity introduced by reflections from the end of the daughter tube. The daughter tubes were connected with the mother tube to form six sets, providing three positive and three negative reflection coefficients. For example, set A indicates the connection of mother tube with daughter tube A. The details of the daughter tubes used in this work are shown in Table 1. Daughter tubes A, B, C, and D were connected directly to the mother tube by overlapping ~1 cm length of the inlet of each daughter tube over the outlet of the mother tube and no connector was used. Daughter tubes E, F were connected to the mother tube by overlapping the inlet of each over a short connecting tube of ~2 cm length, which in turn was connected to the mother tube, also through overlapping. The mother tube and each of the daughter tubes are uniform in both dimension and mechanical properties along its length. The mother tube was fully immersed in a water tank, where the water level was approximately 1 cm above its upper wall. All tubes were kept in the horizontal position.

2.1.2. Pump

The inlet of the mother tube was connected to a piston pump, which generated a reproducible approximately semi-sinusoidal single pulse wave with the piston moving forward from the bottom to top dead centre. The cylinder of the pump is 5 cm in diameter and the stroke of the piston is 2 cm; giving a displaced volume of approximately 40 ml.

2.1.3. Reservoirs

The inlet of the mother tube and outlet of each of the daughter tubes were connected to an inlet and outlet reservoirs, respectively. The inlet and outlet reservoirs were connected and the height of the fluid in the reservoirs was adjusted to 10 cm above the longitudinal axis of the tube; producing an initial hydrostatic pressure of 1 kPa. The differences in mean transmural pressure for different-sized tubes were negligible. A one-way valve was placed between the outlet of reservoir

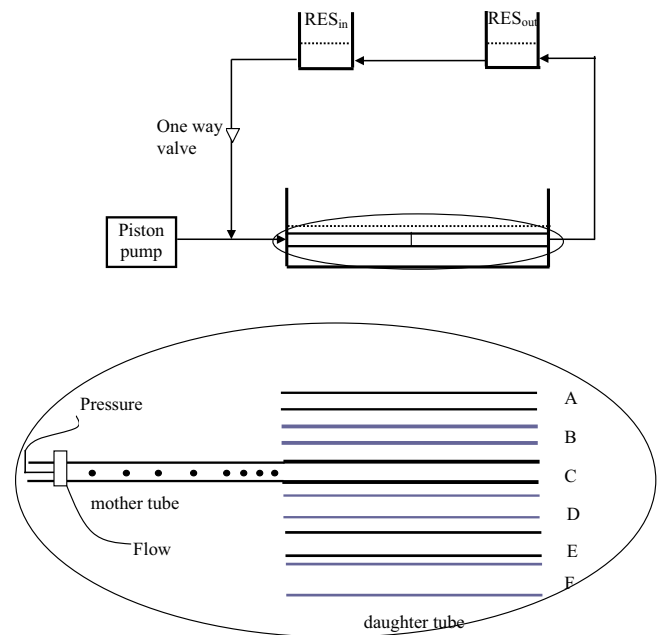


Fig. 1. A schematic diagram of the experimental setup. RES_{inlet} and RES_{outlet} are the inlet and outlet reservoirs which provided the initial pressure to the system, and kept the tube free of air. Pressure and flow were measured using transducer tipped catheters, and ultrasonic flow metre and probes, respectively. All elements of the experiment are placed on the horizontal plane so that the heights of the inlet and outlet reservoirs were equal.

Table 1

Daughter tubes properties and reflection coefficients. D_{in} : internal diameter, h : wall thickness, R_t : theoretical reflection coefficient and C : wave speed in daughter tubes.

| Set | D_{in} (mm) | h (mm) | Material | R_t | C (m/s) |
|-----|---------------|----------|----------|-------|-----------|
| A | 8 | 2 | Silicone | +0.36 | 25.52 |
| B | 8 | 1 | Silicone | +0.28 | 22.27 |
| C | 10 | 2 | Silicone | +0.12 | 25.30 |
| D | 12 | 1 | Silicone | -0.12 | 22.27 |
| E | 16.7 | 1.5 | Rubber | -0.39 | 23.89 |
| F | 21 | 1.5 | Rubber | -0.60 | 20.73 |

and inlet of the mother tube, as shown in Fig. 1, to ensure the whole of the displaced volume flowed into the mother tube.

2.1.4. Measurements

Simultaneous pressure and flow waveforms were measured at the same axial locations in the mother tube. Because the pressure catheter was only 1.2 m long, measurements were made every 10 cm from the inlet via the inlet connection and every 10 cm from the outlet via the outlet connector. Additional measurements were made every 5 cm in the 20 cm closest to the reflection site at the outlet of the mother tube. For each measurement of pressure and flow in the mother tube, the pressure was also measured in the daughter tube 10 cm downstream of the reflection site using another pressure catheter introduced through the Y junction connector, no stopcock in the connector.

Pressure and flow were measured respectively using a 6F pressure transducer tipped catheter (Millar Instruments Inc., Houston, Texas, USA) and ultrasonic flow probe (Transonic System, Inc, Ithaca, NY, USA). External diameter and wall thicknesses of the tubes were measured using a digital caliper. All the data were acquired at a sampling rate of 500 Hz using Sonolab (Sonometrics Corporation, London, Ontario, Canada). Data analysis was carried out using programs written in Matlab (The Mathworks, Natick, MA, USA).

2.2. Theoretical reflection coefficient

For flexible tubes and arteries where the flow velocity (U) is generally much lower than the wave speed (c), the theoretical reflection coefficient (R) of a junction is a function of the sectional area (A), and wave speed (c) of the mother and the daughter tubes, and the fluid density. For a single junction R can be calculated as

$$R_t = \frac{1/Z_0 - 1/Z_1}{1/Z_0 + 1/Z_1} \quad (1)$$

where Z is the impedance of the vessel, $Z = \frac{\rho c}{A}$, ρ is fluid density. Subscript 0 indicates the mother and 1 the daughter tube. Assuming that the test liquid is incompressible, this reduces to

$$R_t = \frac{A_0/c_0 - A_1/c_1}{A_0/c_0 + A_1/c_1} \quad (2)$$

2.3. Wave intensity analysis

Wave intensity analysis considers a waveform to be made of infinitesimal wave fronts (Parker and Jones, 1990) and the intensity carried by the wave can be calculated as

$$dI = dP dU \quad (3)$$

where dP and dU are respectively the pressure and velocity changes across the wave front. If c and ρ are known, dI can be separated into the forward (+) and backward (-) intensities using dP and dU calculated from the measured P and U ,

$$dI_{\pm} = \pm \frac{1}{2\rho c} (dP \pm \rho c dU)^2 \quad (4)$$

The energy carried by forward (+) and backward (-) running waves can be obtained by integrating Eq. (4) over the duration of the wave.

$$I_{\pm} = \int_0^T dI_{\pm} dt \quad (5)$$

where T is the duration of the wave. An example of the measured pressure and calculated wave intensity is shown in Fig. 2.

2.4. Calculation of reflection coefficients

We tested 5 different techniques of calculating the reflection coefficient

- 1) R_{dP} – ratio of peak pressures

The ratio of net changes of peak backward (ΔP_-) to forward (ΔP_+) pressure waves,

$$R_{dP} = \frac{\Delta P_-}{\Delta P_+} \quad (6)$$

where $\Delta P_{\pm} = \sum_{t=0}^T dP_{\pm}$ and $dP_{\pm} = \frac{1}{2}(dP \pm \rho c dU)$ as previously described (Parker and Jones, 1990).

- 2) R_{dI} – ratio of peak wave intensities

The ratio of peak backward wave intensity ΔI_- to peak forward wave intensity ΔI_+ ,

$$R_{dI} = \pm \frac{|\Delta I_-|}{\Delta I_+} \quad (7)$$

- 3) R_I – ratio of net wave energies

The ratio of the net backward wave energy I_- to the net forward wave energy I_+ ,

$$R_I = \pm \frac{I_-}{I_+} \quad (8)$$

The sign of both R_{dI} and R_I is positive (+) if the reflected wave is the same sign as the incident wave and negative (-) if they are different. This definition corresponds to that used by (Mynard et al., 2008).

- 4) $R_{dI}^{0.5}$ – the square root of R_{dI}

Because dI_{\pm} can be written in terms of dP_{\pm}^2 using the water hammer equation,

$$dP_{\pm} = \pm \rho c dU_{\pm} \quad (9)$$

we also considered the reflection coefficient defined as the square root of R_{dI}

$$R_{dI}^{0.5} = \pm \sqrt{\frac{|\Delta I_-|}{\Delta I_+}} \quad (10)$$

- 5) $R_I^{0.5}$ – the square root of R_I

Similarly we considered the reflection coefficient defined as the square root of R_I

$$R_I^{0.5} = \pm \sqrt{\frac{I_-}{I_+}} \quad (11)$$

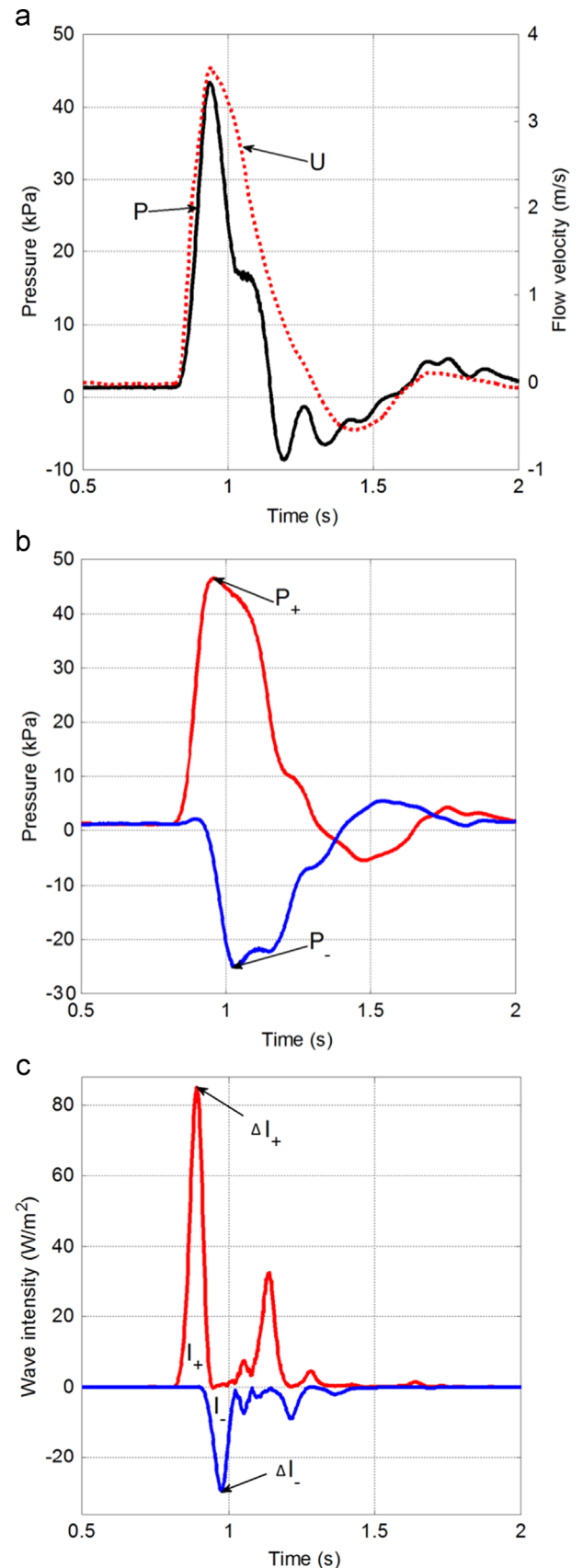


Fig. 2. (a) Raw pressure (solid) and flow velocity (dot) signals measured in set F at 90 cm away from the reflection site. (b) Pressure waveform separation. The arrows show the peak values of the forward (P_+) and backward pressures (P_-). (c) Wave intensity separation. The arrows show the peak values of the forward (ΔI_+) and backward (ΔI_-) wave intensities, the area under the first peak of the wave intensity (dI_+) is the forward wave energy (I_+), and the area under the peak of the backward wave intensity (dI_-) is the backward wave energy (I_-).

Each of the above techniques was used to calculate the reflection coefficient at each of the measurement sites along the mother tube. The average for each technique was calculated as the mean of all values determined along the mother tube.

2.5. Transmission coefficient

The transmission coefficient T is simply related to the reflection coefficient (Stergiopoulos et al., 1996).

$$T = 1 + R \tag{12}$$

2.6. Analysis

Data were collected twice at each measurement site to ensure reproducibility, and the reported results are the mean values. Wave speed c of the mother tube is 20.2 m/s, which was determined by the foot-foot method and confirmed by compliance and mechanical tests.

3. Results

3.1. Wave separation

3.1.1. Pressure waveform separation

Fig. 3a and b show the peaks of separated forward and backward pressures as a function of distance from the reflections site $x=0$ for $R_t=0.36$ and -0.60 . Peak P_+ decreases exponentially as the pulse wave travels towards the reflection site. When the pulse wave is reflected and travels back towards the inlet of the mother tube, peak P_- also decreases exponentially.

It is seen that the peaks of P_+ have almost the same magnitude in both setups, and the equations describing the decay have similar exponential terms. This is because the forward pressure wave is related to the pump, which generates the pulse wave and the

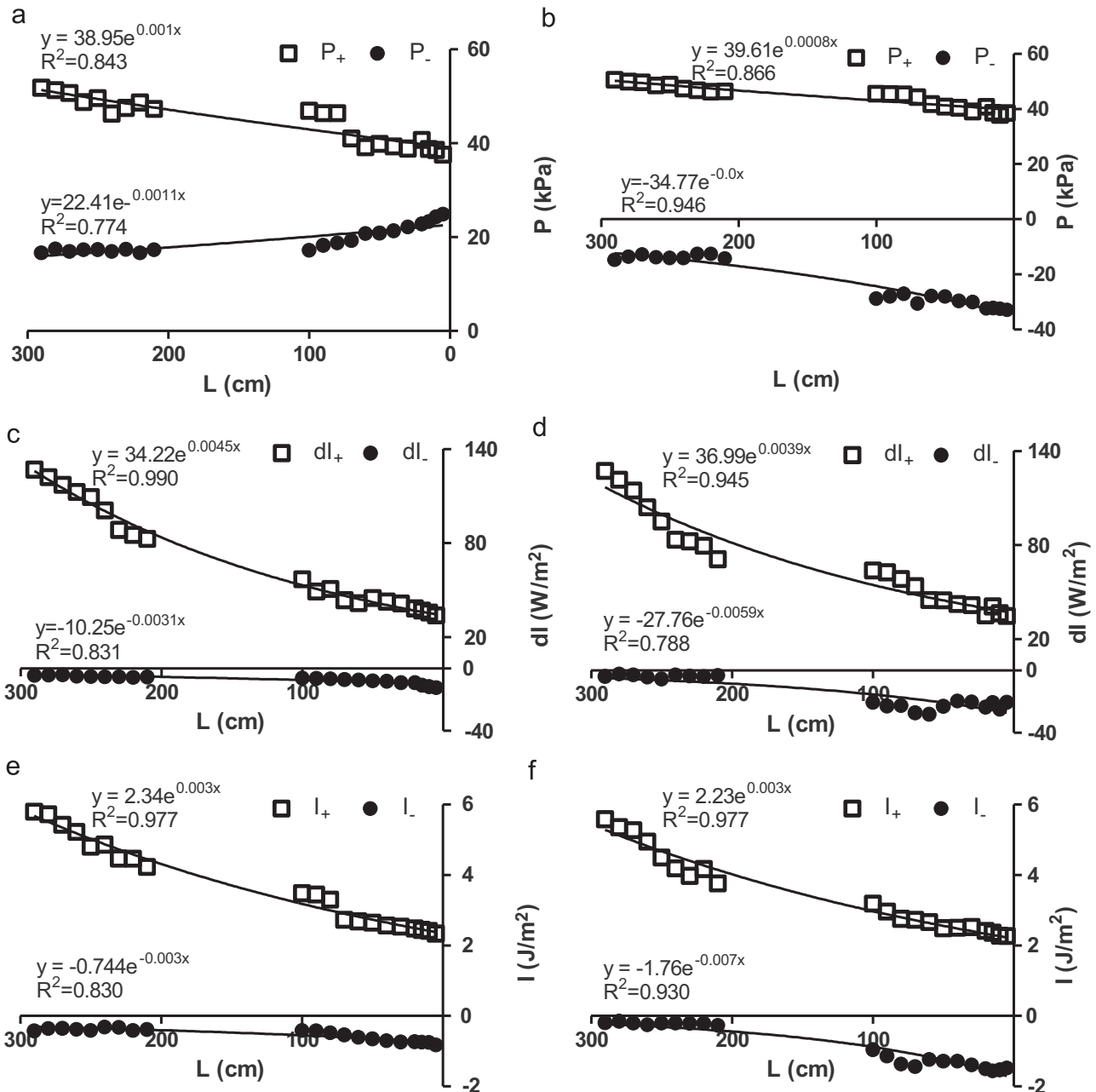


Fig. 3. Wave separation for sets A and F. (a) and (b) are the pressure separation, (c) and (d) are the wave intensity separation, (e) and (f) show the wave energy separation. The solid lines indicate exponential fits to the measured parameters with the parameters given in the figure. $L=0$ cm is the location of the reflection site, the junction of the mother and daughter tube.

mechanical properties of the mother tube, but not affected by the reflection. The peak of P_- varies with different daughter tubes, since they present different reflection coefficients. For positive and negative reflection coefficients, P_- is positive and negative, respectively.

3.1.2. Separation of wave intensity and wave energy

The peak of wave intensity, dl_{\pm} , and wave energy, I_{\pm} , for sets A and F are shown in Fig. 3c–f. dl_{\pm} and I_{\pm} follow similar patterns to that of pressure waves. The exponential decays dl_+ and I_+ show similarity in sets A and F, however, dl_- and I_- are dissimilar between the two tubes due to the different reflection coefficients, shown in Fig. 3c–f. To appreciate the pattern of differences between the two sets, the normalised P_- , dl_- and I_- are shown respectively in Fig. 4a–c. The exponential equations of the curve fitting and correlation coefficient (r^2) are shown in Table 2.

3.2. Mean reflection coefficient

Fig. 5 shows mean values (average of all the measurement sites) of the local reflection coefficients R_{dlp} , $R_{dl}^{0.5}$, $R_l^{0.5}$, R_{dl} , and R_l along each tube plotted when R_t is varied between -0.60 and 0.36 . The results of mean values of R_{dlp} , $R_{dl}^{0.5}$ and $R_l^{0.5}$ are very close to each other, and close to the theoretical reflection coefficient, R_t . Mean values of R_{dl} and R_l are very close to each other, but far from R_t .

The values of mean and local reflection coefficient measured closest to the reflection site are also shown in Table 3, where the differences between the five approaches and the theoretical reflection coefficients are calculated.

3.3. Local reflection coefficient

Fig. 6 shows the local reflection coefficients for all the tubes. Values of the calculated local reflection coefficients are increasing as the measurement site is closer to the reflection site with the positive reflections, and decreasing with the negative reflections. Results of the R_{dlp} , $R_{dl}^{0.5}$ and $R_l^{0.5}$ are very close to each other at each measurement site in each tube. Results of R_{dl} and R_l are close to each other, and their values close to the reflection site are very close to R_t . Table 3 shows the local reflection coefficient close to the reflection site of all the approaches, and the differences between the local reflection coefficient and theoretical values. For example, local values of R_{dlp} , $R_{dl}^{0.5}$ and $R_l^{0.5}$ close to the reflection in set A are much bigger than R_t (values 0.66 , 0.60 and 0.59 are 83.33% , 66.67% and 63.89% bigger than 0.36), the local values of R_{dl} and R_l (0.36 and 0.35) are closer to R_t . In set E, R_{dl} and R_l values -0.33 and -0.36 are the closest to R_t (-0.39), differences are -15.38% and -7.69% respectively, much smaller than the values of R_{dlp} , $R_{dl}^{0.5}$ and $R_l^{0.5}$ (-0.59 , -0.58 and -0.60).

3.4. Transmission coefficient

In order to examine the internal consistency of the experiments, the transmission coefficient was calculated using Eq. (12). Table 4 shows the theoretical transmission coefficient for all the tubes, using Eq. (12) and R_t . Also is shown the calculated transmission coefficient, where R was determined using dl_+ and dl_- and Eq. (4) close to the reflection site from. For example, set A, peak dl_+ is 33.7 W/m^2 , peak dl_- is -12.27 W/m^2 indicating a reflection coefficient of 0.36 and a transmission coefficient of 1.36 ; same as the theoretical value. The experimental and theoretical results are in good agreement.

4. Discussion

In this experimental study, we investigated whether local WIA measurements can be used to determine the local reflection

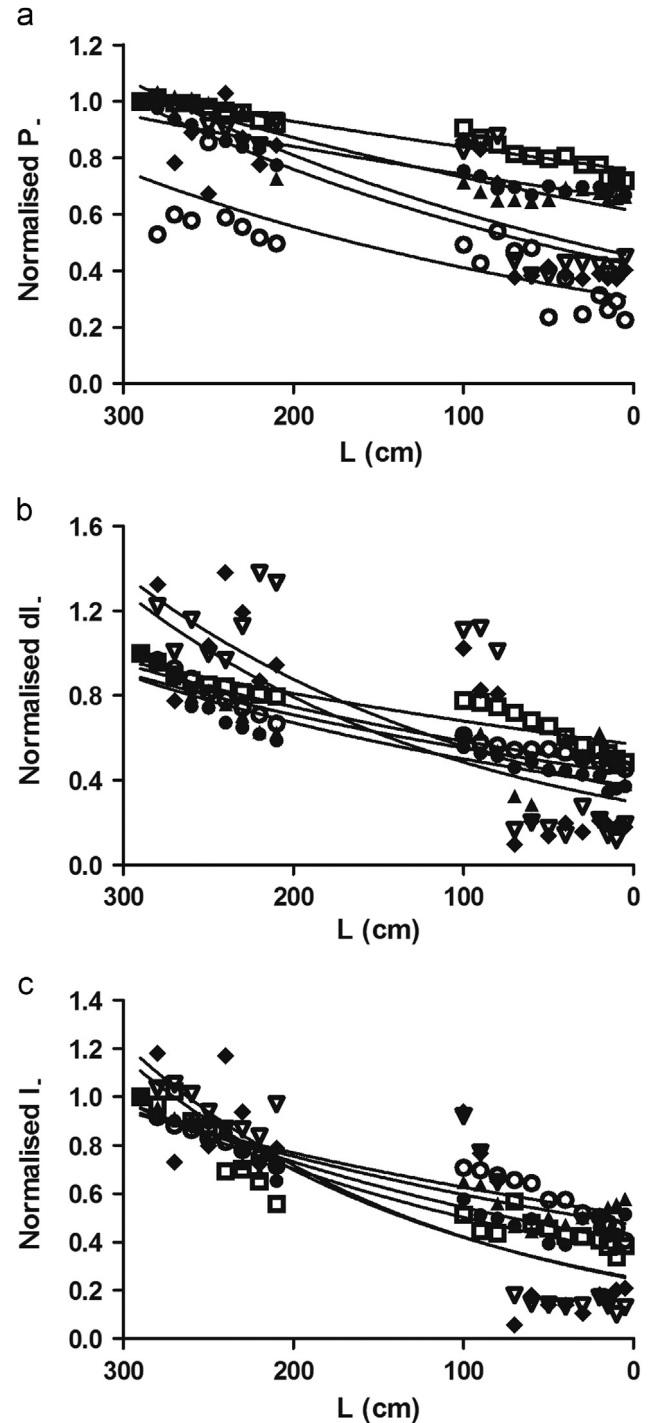


Fig. 4. Normalised backward pressures, wave intensities and energies against distance to reflection site in all tubes, by R_{dlp} (\bullet), $R_{dl}^{0.5}$ (Δ), $R_l^{0.5}$ (\circ), R_{dl} (\blacktriangledown), and R_l (\square). $L=0 \text{ cm}$ is the location of the reflection site, the junction of the mother and daughter tube.

coefficient. R_{dlp} , $R_{dl}^{0.5}$, $R_l^{0.5}$, R_{dl} , and R_l are the five techniques used in this study to calculate the local reflection coefficient, and their results are compared with the theoretical reflection coefficient. The results show that the reflection coefficients determined by all of the techniques increased or decreased, depending on the type of the reflection site, as the measurement site moved towards the reflection site. Values of R_{dl} and R_l measured close to the reflection site are similar to the theoretical values, while values of R_{dlp} , $R_{dl}^{0.5}$, and $R_l^{0.5}$ overestimate the theoretically calculated local reflection coefficient.

Our results indicate that mean values of R_{dp} , $R_{dl}^{0.5}$ and $R_l^{0.5}$ are close to R_t , whilst R_{dl} and R_l are smaller than R_t (Fig. 5). The mean value of reflection coefficient accounts for all the reflections downstream the inlet of the mother tube in vitro. In their computational work Mynard et al. (2008) reported that under linear flow conditions, the square root of the magnitude of dl-derived coefficients, $R_{dl}^{0.5}$ and $R_l^{0.5}$ (power-type) are equal to the pressure-derived coefficient R_{dp} (pressure-type) and they are all equal to the

theoretical coefficient R_t , although the absolute values of R_{dl} and R_l are smaller. We argue that applying the square root to R_{dl} and R_l , $R_{dl}^{0.5}$ and $R_l^{0.5}$ could also be considered as the ‘pressure-type’ coefficients. Using the water hammer Eq. (9), net wave intensity, $dl = dPdU$, can be presented as $dl = dP^2/\rho c$, and Eq. (8) could be rewritten as $R_{dl} = (dP_-^2/\rho c)/(dP_+^2/\rho c)$, and $R_{dl}^{0.5} = dP_-/dP_+$. The same argument could also be applied to $R_l^{0.5}$. This approach explains why the values of R_{dl} and R_l are not comparable to R_{dp} , but values of $R_{dl}^{0.5}$ and $R_l^{0.5}$ are, which is in agreement with the experimental results.

As the measurement site approaches the reflection site, the local reflection coefficient increases for the positive reflections (Fig. 6a–c) and decreases for the negative reflections (Fig. 6d–f). The values of local reflection coefficients determined by wave intensity and wave energy close to the reflection site reached the theoretical reflection coefficients, the differences being less than 5%. These results clearly show that the local reflection coefficient is not the same along the tube, being smaller far from the reflection site. This result can be explained by considering wave dissipation. The peak of P_+ , dl_+ and I_+ decreased exponentially as the wave travelled forward (towards the reflection site), and similarly P_- , dl_- and I_- decreased exponentially in the backward direction (towards the inlet). These results are in agreement with earlier experimental work in similar

Table 2
Wave dissipation in all tubes.

| Set | | P_- | dl_- | I_- |
|-----|----------|----------------|----------------|----------------|
| A | Exponent | $e^{-0.0011x}$ | $e^{-0.0027x}$ | $e^{-0.0027x}$ |
| | r^2 | 0.774 | 0.867 | 0.795 |
| B | Exponent | $e^{-0.0011x}$ | $e^{-0.0019x}$ | $e^{-0.0029x}$ |
| | r^2 | 0.958 | 0.918 | 0.755 |
| C | Exponent | $e^{-0.0015x}$ | $e^{-0.0024x}$ | $e^{-0.0021x}$ |
| | r^2 | 0.693 | 0.594 | 0.766 |
| D | Exponent | $e^{-0.0033x}$ | $e^{-0.0022x}$ | $e^{-0.0022x}$ |
| | r^2 | 0.749 | 0.855 | 0.902 |
| E | Exponent | $e^{-0.0037x}$ | $e^{-0.008x}$ | $e^{-0.0081x}$ |
| | r^2 | 0.910 | 0.868 | 0.812 |
| F | Exponent | $e^{-0.0037x}$ | $e^{-0.0084x}$ | $e^{-0.0088x}$ |
| | r^2 | 0.937 | 0.891 | 0.957 |

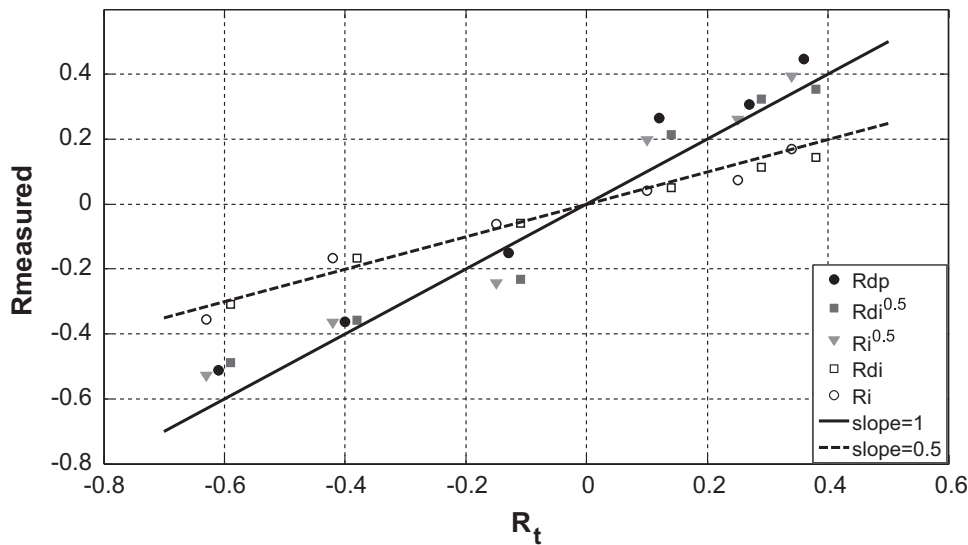


Fig. 5. The mean values of local reflection coefficients in all sets compared to the theoretical reflection coefficient. The values of R_t are -0.60 , -0.39 , -0.12 , 0.12 , 0.28 and 0.36 , respectively shown in the x axis. Values for the reflection coefficients based on dl and I have been displaced by the size of the markers on the x-axis for clarity.

Table 3
Mean and local reflection coefficient (nearest to the reflection site) calculated by 5 techniques. The difference between each technique and the theoretical R is calculated as: $\text{diff}\% = 100\% \times (R - R_t) / R_t$ and shown in brackets.

| Set | R_t | R_{dp} | | $R_{dl}^{0.5}$ | | $R_l^{0.5}$ | | R_{dl} | | R_l | |
|-----|-------|-------------------------------|--------------------|-------------------------------|--------------------|-------------------------------|--------------------|-------------------------------|--------------------|-------------------------------|-------------------|
| | | Mean \pm SD | Local | Mean \pm SD | Local |
| A | 0.36 | 0.45 ± 0.11 (25.00%) | 0.66 (83.33%) | 0.35 ± 0.13 (-2.78%) | 0.60 (66.67%) | 0.39 ± 0.12 (12.42%) | 0.59 (63.89%) | 0.14 ± 0.10 (-61.11%) | 0.36 (0%) | 0.17 ± 0.10 (-52.78%) | 0.35 (-2.78%) |
| B | 0.28 | 0.30 ± 0.09 (7.14%) | 0.40 (42.86%) | 0.32 ± 0.10 (14.29%) | 0.50 (78.57%) | 0.26 ± 0.08 (-7.14%) | 0.49 (75.00%) | 0.11 ± 0.06 (-60.71%) | 0.25 (-10.71%) | 0.12 ± 0.07 (-57.14%) | 0.24 (-14.29%) |
| C | 0.12 | 0.27 ± 0.08 (125.00%) | 0.38 (216.67%) | 0.21 ± 0.07 (75.00%) | 0.33 (175.00%) | 0.20 ± 0.05 (66.67%) | 0.30 (150.00%) | 0.05 ± 0.03 (-58.33%) | 0.11 (-8.33%) | 0.04 ± 0.02 (-66.67%) | 0.09 (-25.00%) |
| D | -0.12 | -0.15 ± 0.07 (25.00%) | -0.35 (191.67%) | -0.23 ± 0.07 (91.67%) | -0.34 (183.33%) | -0.24 ± 0.06 (100.00%) | -0.37 (208.33%) | -0.06 ± 0.04 (-50.00%) | -0.11 (-8.33%) | -0.6 ± 0.03 (-50.00%) | -0.14 (16.67%) |
| E | -0.39 | -0.36 ± 0.17 (-7.69%) | -0.59 (51.28%) | -0.36 ± 0.20 (-7.69%) | -0.58 (48.72%) | -0.36 ± 0.19 (-7.69%) | -0.60 (53.85%) | -0.17 ± 0.14 (-56.41%) | -0.33 (-15.38%) | -0.17 ± 0.13 (-56.41%) | -0.36 (-7.69%) |
| F | -0.60 | -0.54 ± 0.24 (-10.00%) | -0.85 (41.67%) | -0.49 ± 0.27 (-18.33%) | -0.77 (28.33%) | -0.50 ± 0.27 (-16.67%) | -0.81 (35.00%) | -0.31 ± 0.25 (-48.33%) | -0.59 (-1.67%) | -0.36 ± 0.29 (-40.00%) | -0.65 (8.33%) |

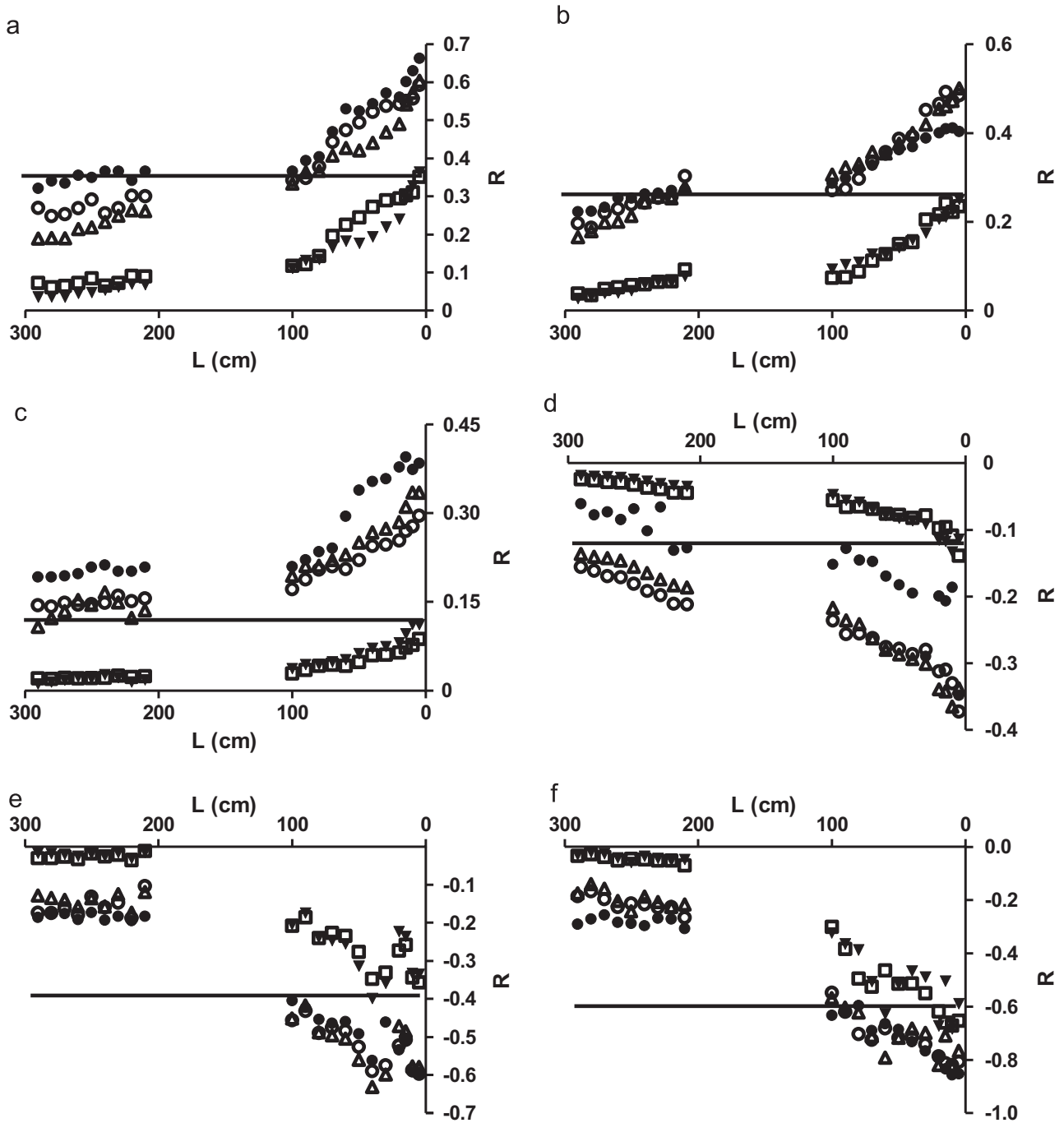


Fig. 6. Local reflection coefficients determined by R_{dl} (●), $R_{dl}^{0.5}$ (Δ), $R_l^{0.5}$ (○), R_{dl} (▼), and R_l (□) for all tubes. The values of R_t are a) 0.36, b) 0.28, c) 0.12, d) -0.12 , e) -0.39 and f) -0.60 . The solid horizontal lines show the values of R_t .

flexible tubes (Feng et al., 2007). Further, Fig. 4 and Table 2 show that the exponential decay associated with the three positive reflections is similar, and likewise for the exponential decay associated with the three negative reflections. However, the exponential decay of the negative reflections is bigger than those of the positive reflections. These findings agree with those reported by Feng and Khir's (2008), where they concluded that the dissipation of the expansion wave was greater than that of the compression wave.

As shown in Fig. 3, separated pressure, wave intensity and energy are decreasing exponentially along the wave travel direction. Therefore, the largest and smallest values of the local reflection coefficients are present, respectively, at the nearest and furthest measurement site nearest and furthest to the reflection site. The present experimental

results are not in agreement with earlier computational work (Mynard et al., 2008), in which the authors argued that under non-linear flow conditions compression waves amplify as they propagate, the R_{dl} and R_l are greater than R_t with compression reflection. They also argued that changes in wave peaks are expected to be negligible when wave speed is high or vessel cross-sectional area is small. Compared to their extreme reflection models ($R=1$ or -1), wave speed is 3.27 m/s and sectional area is 4 cm²; the sectional area of the mother tube in our experiments is 1 cm², and wave speed of 20.2 m/s. The different properties might explain the difference between the experimental and computational results.

The results of the current experiments showed that R_{dl} overestimated R_t , which was somewhat surprising. A possible

explanation is that as the wave crosses the reflection site, the front of the wave is reflected whilst the back of the wave is yet to be reflected. Hence, an increase in pressure is possible due to the coincidence of the two parts of the wave. This may increase the magnitude of the reflected wave, and consequently the reflection coefficient. This is illustrated in Fig. 7 which is a sketch that shows a forward-travelling half-sine wave pressure pulse generated 6 m from the reflection site at $x=0$, where we considered the reflection coefficient is 0.5 and the transmission coefficient is 1.5. Close to the

Table 4

The reflection and transmission coefficients calculated using the pressure and wave intensity approaches from measurements closest to the reflection site. (A) T_t and T_{dl} indicate respectively the transmission coefficient's theoretical value and that determined experimentally using wave intensity. T_t and T_{dl} are in good agreement, with the exception of tube E, their differences in all the tubes are within the experimental error and $< \pm 3\%$. R_{dl} is also in good agreement with the theoretical value (Table 1). (B) The reflection (R_{dp}) and transmission (T_{dp}) coefficients determined using P_+ and P_- are not in agreement with R_t and T_t with large differences.

| (A) | | | | | |
|-----|----------------------------|----------------------------|----------|---------------|-------------------|
| Set | Mother tube | | | Daughter tube | |
| | dl_+ (W/m ²) | dl_- (W/m ²) | R_{dl} | $T_t=1+R_t$ | $T_{dl}=1+R_{dl}$ |
| A | 33.70 | -12.27 | 0.36 | 1.36 | 1.36 |
| B | 31.09 | -7.78 | 0.25 | 1.28 | 1.25 |
| C | 35.96 | -4.03 | 0.11 | 1.12 | 1.11 |
| D | 42.35 | -4.83 | -0.11 | 0.88 | 0.89 |
| E | 34.85 | -11.67 | -0.33 | 0.61 | 0.67 |
| F | 34.59 | -20.37 | -0.59 | 0.4 | 0.41 |

| (B) | | | | | |
|-----|-------------|-------------|----------|---------------|-------------------|
| Set | Mother tube | | | Daughter tube | |
| | P_+ (kPa) | P_- (kPa) | R_{dp} | $T_t=1+R_t$ | $T_{dp}=1+R_{dp}$ |
| A | 37.59 | 24.92 | 0.66 | 1.36 | 1.66 |
| B | 38.62 | 15.60 | 0.40 | 1.28 | 1.40 |
| C | 37.45 | 14.41 | 0.38 | 1.12 | 1.38 |
| D | 41.88 | -7.96 | -0.19 | 0.88 | 0.81 |
| E | 40.36 | -23.98 | -0.59 | 0.61 | 0.41 |
| F | 39.51 | -33.58 | -0.85 | 0.4 | 0.15 |

reflection site the reflected wave generated by the early parts of the incident wave overlap with the later parts of the incident wave creating a summation wave. Sufficiently far from the reflection site, the incident and reflected waves separate in time. The pressure waveforms measured at the 3 locations indicated by the shaded planes are shown by the thick lines. At $x=0$, the two waves coincide giving a single half-sine waveform with magnitude 1.5. At approximately 2 m from the reflection site, the waveform of the summation wave is surprisingly complex. At approximately 4 m from the reflection site the forward and backward waves separate and exhibit half-sine waveforms with amplitudes 1 and 0.5. This sketch shows that the calculation of the reflection coefficient is straightforward if the incident and reflected waves are separate and dissipation is negligible, but less straightforward in the zone where the waves overlap producing a fairly complex waveform. In our experiment the mother tube is shorter than the length of the pulse wave, as it is in the aorta, and separation of the incident and reflected wave requires some signal analysis which can introduce errors into the determination of the reflection coefficient.

Khair and Parker (2002) used WIA to study wave reflections and their timing in vitro. Further, magnitude and timing of reflected waves have been studied using WIA in the aorta (Koh et al., 1998; Khir and Parker, 2005), in the coronary arteries (Sun et al., 2003; Davies et al., 2006) and in the carotid artery (Niki et al., 2002). Furthermore, the ratio of Peak dl_- to peak dl_+ has been used in vivo to derive a 'reflection index' in the carotid (Manisty et al., 2009), in the femoral artery (Borlotti et al., 2012) and in the brachial artery (Manisty et al., 2010). The reflection index is an average of all the reflections arising from the numerous reflection sites in vivo, arriving back to the measurement site, as a ratio of the forward wave. The mean reflection coefficient shown in Fig. 5 could resemble the reflection index that is currently being used in vivo as a measure of mean reflections in the arterial system. Although both techniques represent the mean reflections in a given system, we note there is an important difference. Mean value of the reflection coefficients in vitro is determined using multi-measurement sites along the mother tube, however; the reflection index is determined at a single measurement site using the multi-reflections of the multi-branching system of the arterial tree.

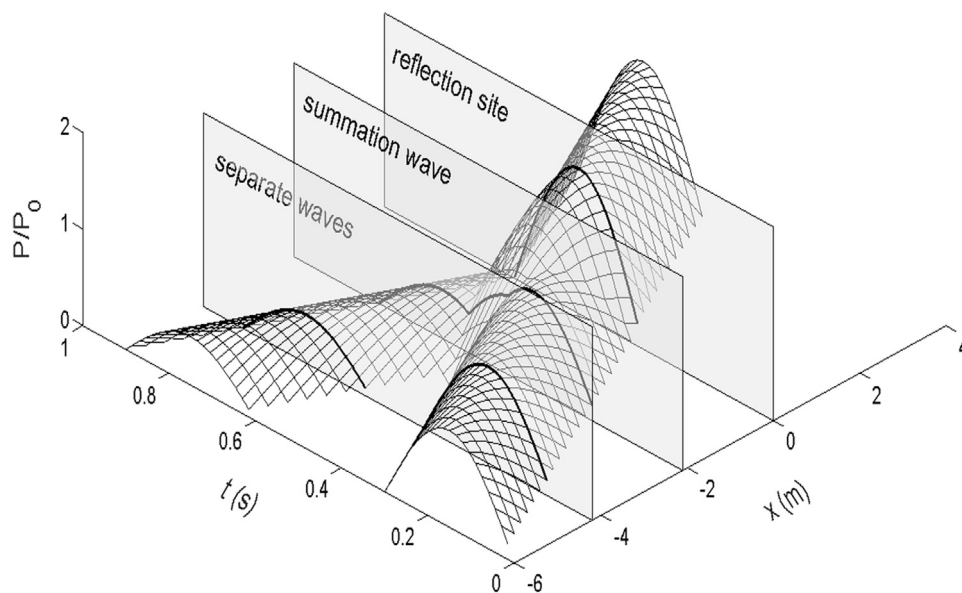


Fig. 7. A sketch that demonstrates the complex waveforms resulting from the interaction of the incident and backward waves. The vertical axis is the pressure waveform normalised with initial pressure. In the mother tube (negative x) close to the reflection site ($x=0$), the temporal waveform (thick lines) is the summation of the backward-travelling reflection of the early part of the wave with the forward-travelling latter part of the wave. Defining the magnitude of the incident and reflected waves in this region can be problematic.

4.1. Experimental and analysis considerations

In attempting to better understand how the waves are reflected and the effect of proximity to the reflection site, we sampled at smaller distances nearer end of the mother tube. We note that including more measurements taken at smaller distances near the reflection site could result in the proximal locations carrying higher weight in determining the mean value. However, the difference obtained by including and excluding the 5 cm measurements is predominantly smaller than the SD of the calculated value; thus we had no reason to exclude any data and our calculations includes the results of all measurements.

4.2. Limitation

This investigation was conducted in a single tube formed by joining two tubes together end to end. In order to isolate other reflections from the reflection generated from the connection of two tubes, the mother and daughter tubes are too long to be considered physiological. Notwithstanding, the arterial system is clearly more complex; a branching system of arteries all shorter than the length of the systolic wave. Therefore the results of the current experiments should be interpreted with caution.

In this study, no measurements were taken in the middle part of the mother tube because of the limited length of the pressure catheter (effective length 1.2 m). This is not expected to influence the interpretations of the results as the first few measurement sites of both upstream and downstream from the no-measurements region are similar.

5. Conclusions

In conclusion, we experimentally demonstrated that the local reflection coefficient can be determined by wave intensity and wave energy along flexible tubes. All five parameters investigated have shown a similar pattern of a reduced measured reflection coefficient as the measurement site moves away from the site of reflection, and this is due to wave dissipation. In our experiments, R_{dl} , $R_{dl}^{0.5}$ and $R_l^{0.5}$ are the most reliable parameters to measure the mean reflection coefficient, whilst R_{dl} and R_l provide the best measure of the local reflection coefficient, closest to the reflection site. Additional work with bifurcations, tapered tubes and in vivo experiments are needed to further understand, validate the method and assess its potential clinical use.

Conflict of interest

The authors have no conflict of interest to report.

References

Borlotti, A., Khir, A.W., Rietzschel, E.R., De Buyzere, M.L., Vermeersch, S., Segers, P., 2012. Noninvasive determination of local pulse wave velocity and wave intensity: changes with age and gender in the carotid and femoral arteries of healthy human. *J. Appl. Physiol.* 113, 727–735.

Davies, J.E., Whinnett, Z.I., Francis, D.P., Manisty, C.H., Aguado-Sierra, J., Willson, K., Foale, R.A., Malik, I.S., Hughes, A.D., Parker, K.H., Mayet, J., 2006. Evidence of a dominant backward-propagating “suction” wave responsible for diastolic coronary filling in humans, attenuated in left ventricular hypertrophy. *Circulation* 113 (14), 1768–1778.

Feng, J., Long, Q., Khir, A.W., 2007. Wave dissipation in flexible tubes in the time domain: in vitro model of arterial waves. *J. Biomech.* 40, 2130–2138.

Feng, J., Khir, A.W., 2008. The compression and expansion waves of the forward and backward flows: an in-vitro arterial model. *Proc. Inst. Mech. Eng. Part H: J. Eng. Med.* 222 (4), 531–542.

Hughes, A.D., Parker, K.H., 2009. Forward and backward waves in the arterial system: impedance or wave intensity analysis? *Med. Biol. Eng. Comput.* 47 (2), 207–210.

Khir, A.W., Parker, K.H., 2002. Measurements of wave speed and reflected waves in elastic tubes and bifurcations. *J. Biomech.* 35 (6), 775–783.

Khir, A.W., Parker, K.H., 2005. Wave intensity in the ascending aorta: effects of arterial occlusion. *J. Biomech.* 38 (4), 647–655.

Khir, A.W., Hughes, A.D., Parker, K.H., 2006. The inflection point is not a reliable method for the determination of the augmentation index. *J. Am. Coll. Cardiol.* 47 (4), 315A.

Khir, A.W., Swalen, M.J.P., Parker, K.H., 2007. The simultaneous determination of wave speed and the arrival time of reflected waves in arteries. *Med. Biol. Eng. Comput.* 45, 1201–1210.

Kips, J.G., Rietzschel, E.R., De Buyzere, M.L., Westerhof, B.E., Gillebert, T.C., Van Bortel, L.M., Segers, P., 2009. Reflection and pulse transit time from the pressure waveform alone. *Hypertension* 53, 142–149.

Koh, T.W., Pepper, J.R., DeSouza, A.C., Parker, K.H., 1998. Analysis of wave reflections in the arterial system using wave intensity: a novel method for predicting the timing and amplitude of reflected waves. *Heart Vessel.* 13, 103–113.

Lekakis, J.P., Ikonomidis, I., Protogerou, A.D., Papaioannou, T.G., Stamatiopoulos, K., Papamichael, C.M., Mavrikakis, M.E., 2006. Arterial wave reflection is associated with severity of extracoronary atherosclerosis in patients with coronary artery disease. *Eur. J. Cardiovasc. Prev. Rehabil.* 13 (2), 236–242.

Lemogoum, D., Flores, G., Van den Abeele, W., Giarka, A., Leeman, M., Degaute, J.P., van de Borne, P., Van Bortel, L., 2004. Validity of pulse pressure and augmentation index as surrogate measures of arterial stiffness during beta-adrenergic stimulation. *J. Hypertens.* 22, 511–517.

Lighthill, J., 1978. *Waves in Fluids*. Cambridge University Press, Cambridge.

Manisty, C., Mayet, J., Tapp, R.J., Parker, K.H., Sever, P., Poulter, N.R., Thom, S.A., Hughes, A.D., 2010. Wave reflection predicts cardiovascular events in hypertensive individuals independent of blood pressure and other cardiovascular risk factors: an ASCOT (Anglo-Scandinavian Cardiac Outcome Trial) substudy. *J. Am. Coll. Cardiol.* 56, 24–30.

Manisty, C.H., Zambanini, A., Parker, K.H., Davies, J.E., Francis, D.P., Mayet, J., Mc, G.T. S.A., Hughes, A.D., 2009. Differences in the magnitude of wave reflection account for differential effects of amlodipine- versus atenolol-based regimens on central blood pressure: an Anglo-Scandinavian Cardiac Outcome Trial substudy. *Hypertension* 54, 724–730.

McEniery, C.M., Yasmin, Hall, I.R., Qasem, A., Wilkinson, I.B., Cockcroft, J.R., 2005. Normal vascular aging: differential effects on wave reflection and aortic pulse wave velocity. *J. Am. Coll. Cardiol.* 46 (9), 1753–1760.

Murgo, J.P., Westerhof, N., Giolma, J.P., Altabelli, S.A., 1980. Aortic input impedance in normal man: relationship to pressure wave forms. *Circulation* 62, 105–116.

Mynard, J., Penny, D.J., Smolich, J.J., 2008. Wave intensity amplification and attenuation in non-linear flow: implications for the calculation of local reflection coefficients. *J. Biomech.* 41, 3314–3321.

Nichols, W., O'Rourke, M., 2005. *McDonald's Blood Flow in Arteries. Theoretical, Experimental and Clinical Principles*. Hodder Arnold – Oxford University Press, USA 2005.

Niki, K., Sugawara, M., Chang, D., Harada, A., et al., 2002. A new non-invasive measurement system for wave intensity: evaluation of carotid arterial wave intensity and reproducibility. *Heart Vessel.* 17, 12–21.

O'Rourke, M.F., Mancia, G., 1999. Arterial stiffness. *J. Hypertens.* 17, 1–4.

O'Rourke, M.F., Hashimoto, J., 2007. Mechanical factors in arterial aging: a clinical perspective. *J. Am. Coll. Cardiol.* 50, 1–13.

Parker, K.H., Jones, C.J.H., 1990. Forward and backward running waves in the arteries: analysis using the method of characteristics. *J. Biomed. Eng.* 112, 322–326.

Segers, P., Rietzschel, E.R., De Buyzere, M.L., Vermeersch, S.J., De Bacquer, D., Van Bortel, L.M., De Backer, G., Gillebert, T.C., Verdonck, P.R., 2007. Noninvasive (input) impedance, pulse wave velocity, and wave reflection in healthy middle-aged men and women. *Hypertension* 49, 1248–1255.

Stergiopoulos, N., Spiridon, M., Pythoud, F., Meister, J.J., 1996. On the wave transmission and reflection properties of stenosis. *J. Biomech.* 29, 31–38.

Sun, Y.H., Anderson, T.J., Parker, K.H., Tyberg, J.V., 2003. Effects of left ventricular contractility and coronary vascular resistance on coronary dynamics. *AJP – Heart Circ. Physiol.* 286 (4), H1590–H1595.

Westerhof, N., Sipkema, P., van den Bos, C.G., Elzinga, G., 1972. Forward and backward waves in the arterial system. *Cardiovasc. Res.* 6, 648–656.

Westerhof, N., O'Rourke, M.F., 1995. Haemodynamic basis for the development of left ventricular failure in systolic hypertension and for its logical therapy. *J. Hypertens.* 13, 943–952.

Westerhof, N., Stergiopoulos, N., Noble, M., 2004. *Snapshots of Hemodynamics. An Aid for Clinical Research and Graduate Education*. Springer Science + Business Media, New York 2004.

Westerhof, B.E., Guelen, I., Westerhof, N., Karamaker, J.M., Avolio, A., 2006. Quantification of wave reflection in the human aorta from pressure alone – a proof of principle. *Hypertension* 48, 595–601.

Yano, M., Kohno, M., Kobayashi, S., Obayashi, M., Seki, K., Ohkusa, T., Miura, T., Fujii, T., Matsuzaki, M., 2001. Influence of timing and magnitude of arterial wave reflection on left ventricular relaxation. *AJP Heart Circ. Physiol.* 280 (4), H1846–H1852.